Comparative Analysis of Structure and Motion of Vision Logistics Robotic Arms

Hongyang Guo *, #, Zhi Gao #

Rongcheng College, Harbin University of Science and Technology, Weihai, China, 264300

* Corresponding author: 15550013755@163.com

#These authors contributed equally.

Abstract. This paper combines visual recognition and robotic arm, optimizes the design of robotic arm structure, and researches the logistics robotic arm with six degrees of freedom and visual perception ability to enrich the logistics robotic use scene. Firstly, the visual recognition system is installed on the existing six-degree-of-freedom robotic arm, and the coordinate system is established by the light bar recognition method combined with the D-H parameter method. Secondly, a kinematic simulation model was established by using MATLAB, and the state of the joints was analyzed by using forward and inverse kinematic simulation and fifth degree polynomial interpolation. Finally, the actual logistics fixed-point transportation task is designed for trajectory planning. The results show that the robotic arm is able to be able to perform different grasping tasks in non-structural environments, around the visual analysis of the robotic arm as well as the optimization of the motion track, to enhance the efficiency of the comprehensive use of visual and tactile information, to improve the adaptability of the robotic hand grasping, and to be able to meet the precise control of the pick-up process and the use of the realization of the payload grasping and dexterous movement. The research in this paper provides a certain reference value for the propulsion robot arm to perform intelligent grasping tasks.

Keywords: Six Degree of Freedom Robotic Arm, Polynomial Interpolation, Visual Identity, Trajectory Planning, Motion Simulation.

1. Introduction

In the logistics industry, the robotic arm occupies a very important position. Traditional manual packaging operations due to labor intensity, low productivity, inconsistent quality and other shortcomings have been unable to meet the needs of people's growing production and life, so the robotic arm with its intelligence, high efficiency, safety and other advantages in the packaging operation has been more and more widely used. Since processes such as gripping and handling are very important for the efficient work of packaging assembly line, the requirements for robotic arms are getting higher and higher.

Many scholars have conducted research in this field. Fu X [1] and others conducted kinematic analysis and trajectory planning of packaging sorting robot based on the standard D-H method, and the results show that the established kinematic equations are correct and feasible, and the data obtained from the simulation can be applied to the motion control of the actual robotic arm to achieve accurate and reliable operation. Zhang Y [2] established a mathematical model of 3D TSP with the shortest path as the optimization objective for the multi-objective apple picking task; elaborated the basic principle of ACO algorithm, and combined it with the multi-objective apple picking task to design an ACO algorithm for apple picking path planning; implemented the apple picking path planning in MATLAB, and analyzed the important parameters of ACO algorithm to obtain reasonable combination; implemented the path planning in VRLAB to obtain reasonable combination; analyzed the important parameters of ACO algorithm in VRLAB to obtain reasonable combination; and analyzed the important parameters of ACO algorithm in VRLAB to obtain reasonable combination. In VREP, a robot arm simulation experiment was carried out for multi-objective apple picking, which verified the feasibility of the robot arm planning path, and at the same time, analyzed the fluctuation of the x,y,z coordinate components at the end of the robot arm, and verified the reasonableness of the above paths in the actual operation. Parikh P et al. [3] investigated a smooth trajectory method for a multi-degree-of-freedom robot using sixth-degree polynomials as an example of a five-degree-of-freedom robot, which can reduce the impact on end-effector and protect the joints from mechanical vibration. GuoW et al. [4] proposed a capacity algorithm for a five-degree-of-freedom hybrid robotic arm using a direct method to obtain the optimal trajectory planning and maximum dynamic load. Wang Z et al. [5] used to derive and solve the forward and inverse kinematic equations of the robotic arm using Denavit - Hartenberg (D - H) method and validated it using Robotics Toolbox in Matlab environment, and then used Monte Carlo method to perform the workspace analysis, and finally The Robotics Toolbox is used to simulate and analyze the motion planning of Dobot robotic arm for verification. Jia J et al. [6] studied the robotic arm collision avoidance method based on the decision tree algorithm, and the results showed that in complex environments, no collision occurred between the robotic arm and the obstacles in the planned collision avoidance routes, so the method effectively improves the effect of robotic arm collision avoidance. Jin Z et al. [7] and others, based on the electromechanical-hydraulic integration control technology, analyzed and illustrated the structure, principle and technical characteristics of modern robotic arm technology.

In this paper, the current logistics robotic arm faced by the target positioning is not accurate, the position of the package is prone to change due to interference as well as the robot is prone to damage to the package and other problems are comprehensively researched and considered, and a six-degree-of-freedom robotic arm is designed, with a monocular camera and a laser ranging sensor mounted above the clamping jaws, which facilitates the realization of the visual servo control. This not only simplifies the overall structure of the robotic arm, but also avoids collision damage to the sensors in the pickup process. In order to improve the motion accuracy and stability of the robotic arm, its kinematic analysis and trajectory planning is one of the core contents of robotics. In this paper, we take the six-degree-of-freedom robotic arm [8] as the research object, use the improved D-H parameter method [9] to establish the kinematic model of the robotic arm, build the simulation model of the robotic arm and carry out the forward and reverse kinematic analysis by MATLAB, and finally carry out the trajectory planning of the joint space by polynomial interpolation algorithm, and carry out the simulation verification of the actual engineering applications. The tactile sensing and visual sensing [10] in the adaptive grasping process of the manipulator are studied to enhance the adaptive performance of the manipulator grasping.

2. Structural design of Robotic arms

In this paper, the robotic arm adopts the linkage drive of mechanical structure. The connecting rod transmission is based on mechanical design principles to realize power transmission, which has the advantages of good stiffness, large transmission force, high load capacity, high precision and so on. With the development of material technology, the life and quality of the connecting rod material have been reliably guaranteed. Meanwhile, in order to achieve higher flexibility and precision, a six-degree-of-freedom robotic arm is designed. As shown in Figure 1 includes three directions of motion such as rotation, translation, and swivel, and the six axes are as follows: base rotation axis: controls the horizontal rotation of the manipulator and moves it along the horizontal direction. Upper arm rotation axis: controls the manipulator to rotate upward or downward. Elbow rotation axis: controls the elbow joint of the manipulator to rotate. Wrist rotation axis 1: Controls the rotation between the end of the manipulator and the elbow joint. Wrist rotary axis 2: Controls the rotation of the end of the manipulator. End-effector rotary axis: controls the rotation control between the end-effector of the manipulator and the wrist rotary axis 2.

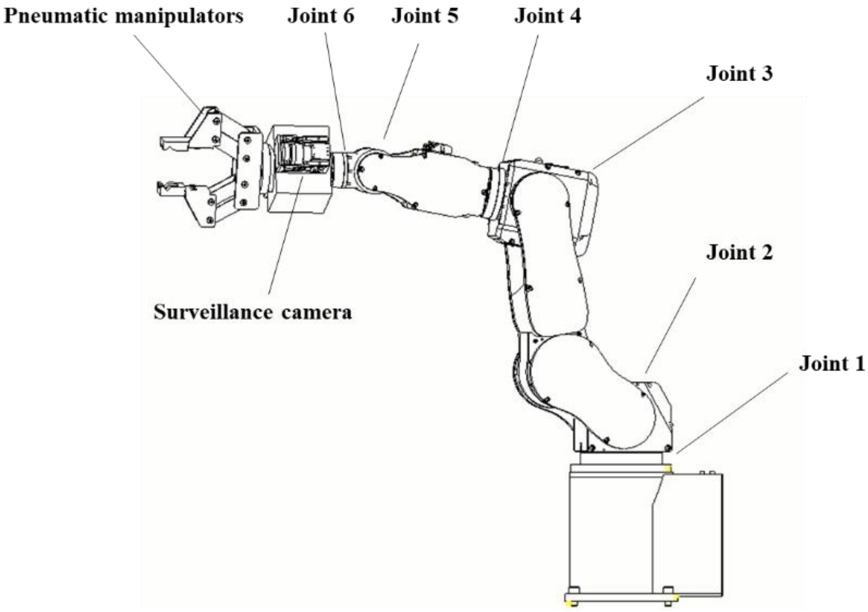

Figure 1. Logistics robot 3D model

The gripper adopts a parallel clamping method and a pneumatic adjustment mechanism [11], as shown in Figure 2. The material selection takes into account the requirements of strength, abrasion resistance, corrosion resistance and light weight. The reasonable structural design of the gripper improves the gripping performance and stability of the mechanical gripper, as well as the precise control and adjustment of the gripping force to ensure the stable gripping of the object, and provides effective support for the structural optimization of the mechanical gripper through modular design and finite element analysis.

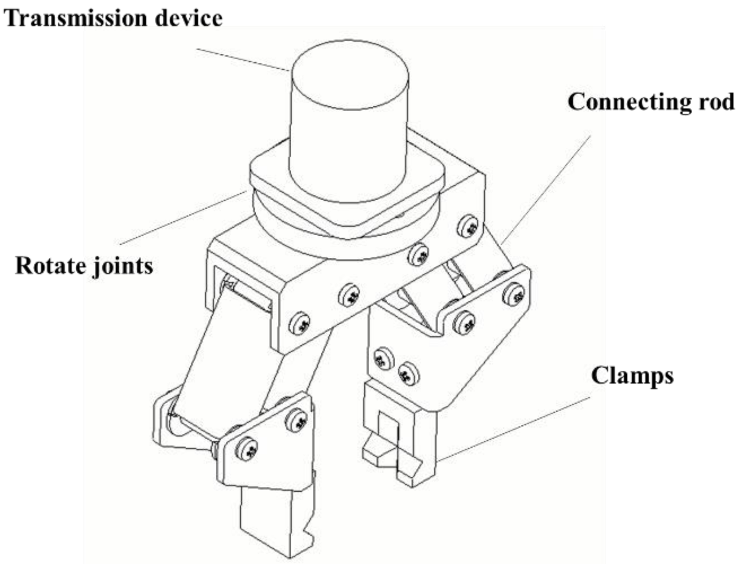

Figure 2. End-effector

The camera is mainly designed with three parts: the lens, CMOS sensor, and the housing. As shown in Figure 3 By improving the lens material and manufacturing, CMOS sensor process, improve the imaging quality of the lens and color reproduction. Selection of high-performance CMOS image sensor to improve image quality and processing speed. Camera housing is mostly made of plastic material, through mold design and optimization to achieve good structural performance and heat dissipation performance.

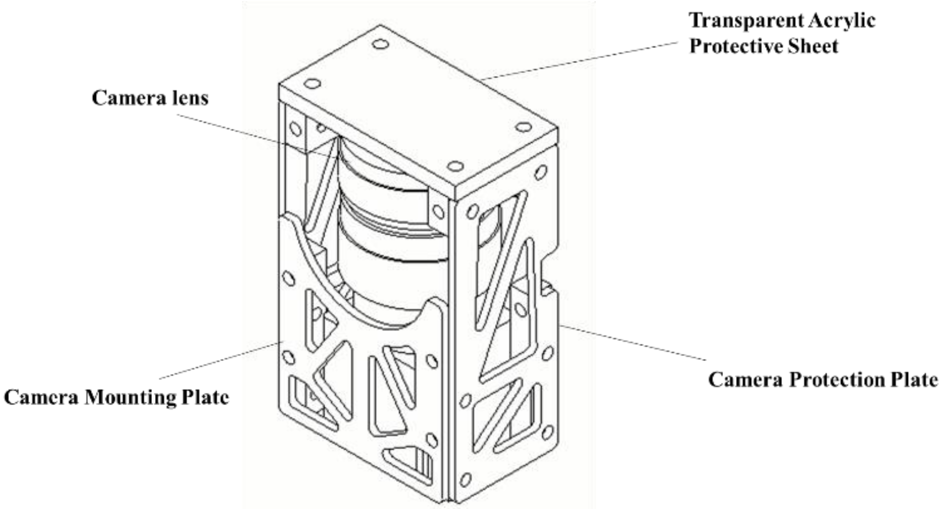

Figure 3. Camcorder

3. Robotic arm visual localization

In this paper, we use light bar recognition and light bar matching [12] for object surface recognition, and use PNP solving to get the final position of the object that needs to be grasped by the relationship between the pixel coordinate system, the world coordinate system and the image coordinate system.

In the actual programming process, the simple and plain recognition algorithm will be affected by many things, so this paper makes several improvements to the plain algorithm. The conventional algorithm is designed to convert the image to HSV image after fetching the stream, and directly carry out the binarization of HSV, and then search for the outer contour of the light bar through OpenCV's find Contours function, but in fact, in the process of running the program, due to the lighting of the actual object and the setting of the camera's exposure time, in order to clearly observe the target, the target's light bar will be overexposed in some distances, showing white color, which is a very important factor in the process of recognition. will be overexposed and appear white, which leads to the inability to obtain the complete light bar contour through HSV binarization, and thus additional expansion and erosion operations are needed in find Contours to make the contours connected, etc., which brings additional time overhead.

Figure 4 depicts this phenomenon, with the result using HSV binarization in the middle and grayscale binarization on the right. While grayscale binarization only observes luminance, in this paper we chose to count the number of red and blue pixels around the contour after grayscale binarization in order to determine the color of the light bar.

Figure 4. Light bar recognition in bad scenes

In the actual operation of the algorithm, the presence of digits between light bars is a strong prior, and accurate digit recognition relaxes the limitations of other hyper-parameters to achieve a higher recognition rate. The digit recognition algorithm is constructed using a simple MLP structure as shown in Figure 5, which supports images of 20x28 pixel size and is trained on the dataset:

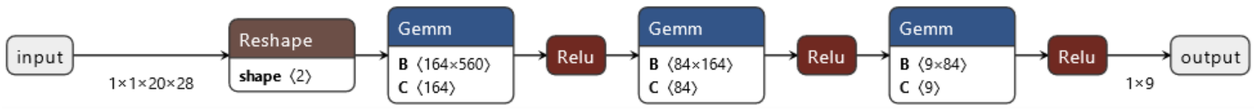

Figure 5. Algorithm drill

The region near the range of the light bar is selected as the ROI and it is transformed into an image that meets the input size of the model using affine transformation, and the image is converted into a binarized picture by adaptive binarization of the Otsu method, and recognition is performed. The pixel coordinate system is obtained X' is the horizontal coordinate of the object to be recognized in the image coordinate system, f is the camera focal length, and X' can be referred to the camera imaging principle as shown in Figure 6:

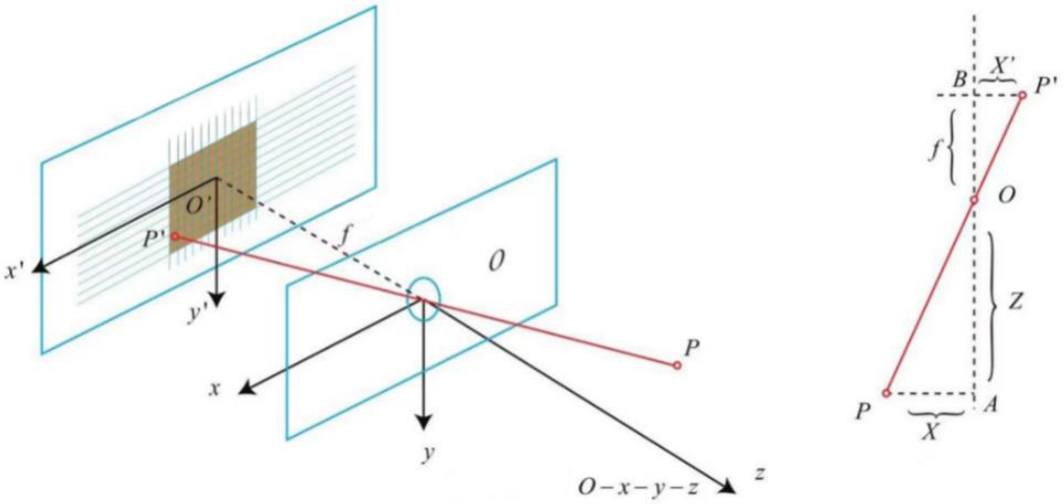

Figure 6. Principles of Camera Imaging

It is known that the coordinates u, v under the pixel coordinate system of the camera is related to X', Y' under the image coordinate system:

$$\begin{cases} u = \alpha X' + c_x \\ v = \beta Y' + c_y \end{cases} \tag{1}$$

u and *v* are the pixel coordinates of the object under the opencv pixel coordinate system, which can be obtained by image processing recognition, and *Cx*,*Cy* are provided by the camera internal reference matrix. However, it is not in the internal reference matrix, so this paper gives another final equation for the camera imaging principle:

$$\begin{cases} u = f_x \frac{X}{Z} + c_x \\ v = f_x \frac{Y}{Z} + c_y \end{cases} \tag{2}$$

Analyzing the above two equations can obtain the visual data for the object surface in the image coordinate system light bar state as well as the position. In order to solve the relationship between pixel coordinates and world coordinates, this paper expands the ordinary image coordinates (*x*, *y*) into spatial coordinates (*x*, *y*, *z*). A point in space, projected onto the image plane is on a straight line with the optical center of the camera, and the camera coordinate system is established with the optical center as the origin. The real coordinates of the object to be picked can be obtained by formula (3).

$$\begin{cases} u = \frac{f \cdot X_c}{Z} \\ v = \frac{f \cdot Y_c}{Z} \end{cases} \tag{3}$$

4. Kinematic analysis of logistics Robotic arms

The research object of this paper is a six-axis manipulator, according to the three-dimensional model of the manipulator Figure1, a simplified robot arm motion model is established in Figure. 7. three-dimensional coordinate system is established at each joint connection, in which the coordinate system 0 is the base coordinate system, the coordinate system 6 is the tool coordinate system which is used to describe the end-effector position in the base coordinate system, and the coordinate systems 4 and 5 coincide. The D-H parameters necessary for the simulation experiments are determined by relating the rotation angle at the joints to the position of the end-effector. The relative position and attitude relationships between the robot's joints can be accurately described by means of four parameters (α, a, d, and θ) that have a clear physical meaning.

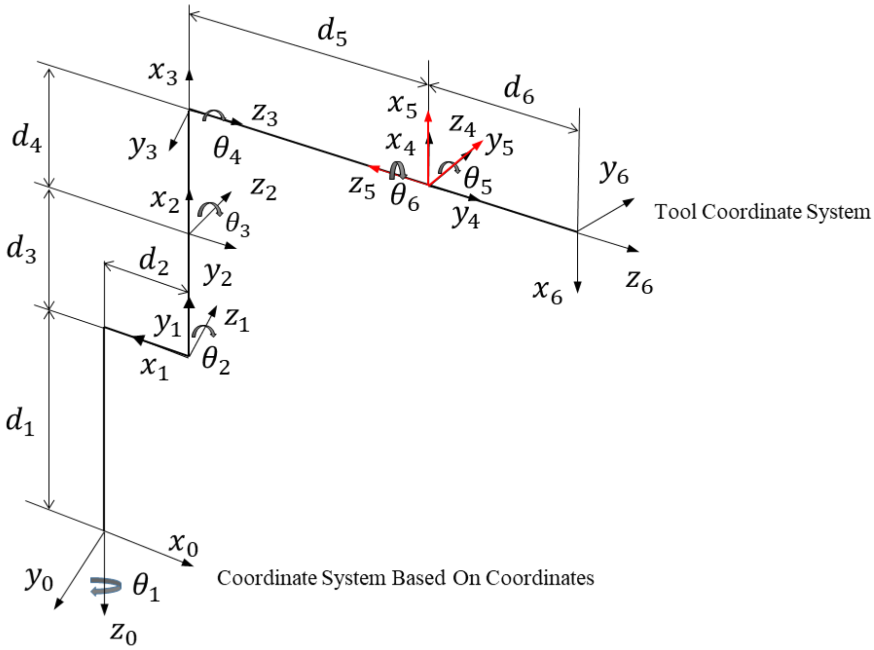

Figure 7. Robotic arm motion model

In this paper, the improved D-H parametric method is used for the definition of the connecting rod coordinate system, which is shown in Figure 8. The axis *z_i* is selected along the direction of joint i; the origin *O_i* is placed at the intersection of the axis *z_i* with the common perpendiculars of the axis *z_(i-1)* and the axis *z_i*; *O_i* is placed at the intersection of the common perpendiculars and the axis *z_(i-1)*; and the axis *y_i* is selected along the common perpendiculars of the axis *z_(i-1)* and *z_i*, in the direction of the direction from joint i pointing to joint i+1; finally, *y_i* is chosen to form a right-handed system. By defining the connecting rod coordinate system, multiple sets of D-H parameters can be obtained as shown in Table 1, which determine the position and direction of coordinate system i and coordinate system i+1 about coordinate system i-1.

The difference between the improved D-H parameter method and the standard D-H parameter method lies in the difference in the establishment of the connecting rod coordinate system and the different multiplication order of the four parameters, which are *α_(i-1)*: the distance from *Z_(i-1)* to *Z_i* along the *X_(i-1)* axis; *a_(i-1)*: the angle from *Z_(i-1)* to *Z_i* along the *X_(i-1)* axis; *θ_i*: the angle from *Z_(i-1)* to *Z_i* along the *Z_i* axis, the angle from *X_(i-1)* to *X_i*; *d_i*: along the *Z_i* axis, the distance from *X_(i-1)* to *X_i* Using *c* and *s* to represent the cosine and sine, the relational equations are shown in Eqs. (4) and (5).

$$ {}^{i-1}_{\ \ i}T = R_X(\alpha_{i-1}) \times D_X(a_{i-1}) \times R_Z(\theta_i) \times D_Z(d_i) \tag{4}$$

$$
{}^{i-1}_{i}T = \begin{bmatrix} c\theta_i & -s\theta_i & 0 & a_{i-1} \\ s\theta_i c\alpha_{i-1} & c\theta_i c\alpha_{i-1} & -s\alpha_{i-1} & -s\alpha_{i-1} d_i \\ s\theta_i s\alpha_{i-1} & c\theta_i s\alpha_{i-1} & c\alpha_{i-1} & c\alpha_{i-1} d_i \\ 0 & 0 & 0 & 1 \end{bmatrix} \quad (5)
$$

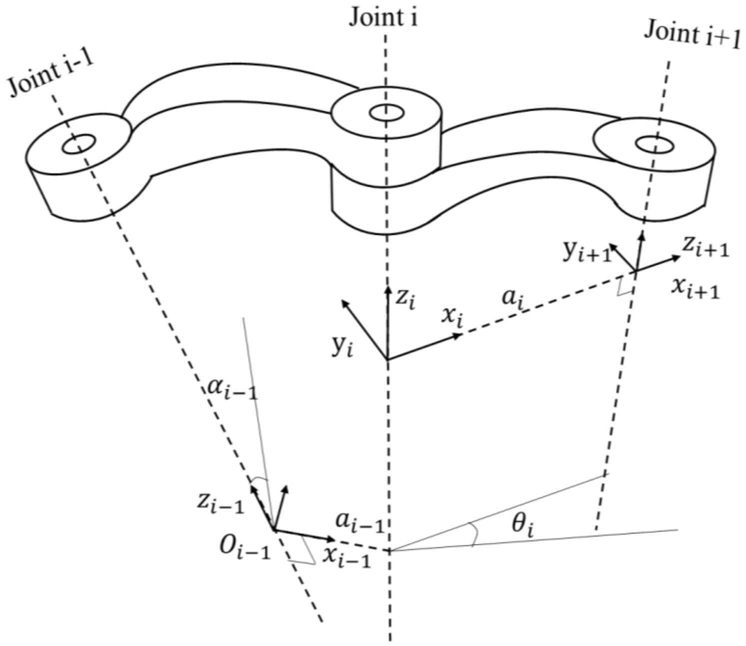

Figure 8. Coordinate system of connecting rods

Table 1. Six Degrees of Freedom Improved D-H Parameters

Link	θ_i	α_{i-1}	a_{i-1}	d_i
1	θ_1	0	0	0.28
2	θ_2	$\pi/2$	0	0.22
3	θ_3	0	0.5	0
4	θ_4	0	0.24	0
5	θ_5	$\pi/2$	0	0
6	θ_6	0	0	0.26

After determining the parameters, the positive kinematic equations are solved according to the inverse of the parameters into the chi-square transformation matrix, i.e., the positive kinematic solution, the transformation matrix of each joint is obtained, and the variables at each joint are obtained, so that the motion of the robotic arm can be determined and simulated. Under the premise of known end-effector position, solve the inverse kinematics equations, i.e., inverse kinematics solution, to get the angle, angular velocity and angular acceleration of the joints, and then obtain the torque of each joint, see Figure 9. through the comparison of the corrections so as to make the robotic arm gripping and positioning more accurate, the formula is shown in Equation (6).

$$
{}^{0}_{6}T = {}^{0}_{1}T\,{}^{1}_{2}T\,{}^{2}_{3}T\,{}^{3}_{4}T\,{}^{4}_{5}T\,{}^{5}_{6}T = \begin{bmatrix} n_x & a_x & o_x & p_x \\ n_y & a_y & o_y & p_y \\ n_z & a_z & o_z & p_z \\ 0 & 0 & 0 & 1 \end{bmatrix} \quad (6)
$$

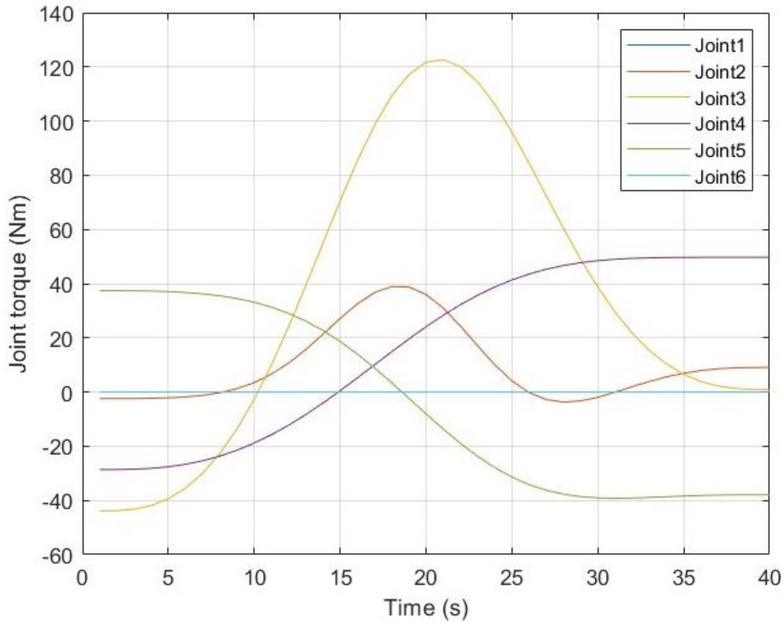

Figure 9. Joint torque variation graph

The moment diagram shows that joint 1, being at the lowest end, is subjected to a large moment and the change is more pronounced. The rest of the five joints, the force situation is similar, the change is smoother. The wear and tear of the joints due to uneven force is effectively avoided, and the motion is more stable.

According to the set D-H parameters, the MATLAB Robotics Toolbox is used to solve the forward and inverse kinematics. Assuming that the start point is [0 0 0 0 0 0 0] and the end point is [0 $3\pi/2$ 0 $3\pi/2$ $\pi/2$ $\pi/2$ $\pi/2$], the kinematic simulation is carried out by solving the position matrices of the initial point and the termination point through the forward kinematics, which is shown in Fig. 10. Then, the inverse kinematics is carried out to solve the position matrix at the initial and termination points, and it is found that the positive kinematic solution is consistent with that of the inverse kinematics, which further verifies the correctness of the D-H parameter setting and simulation model of the robotic arm [12] . parameter setting and simulation model are correct.

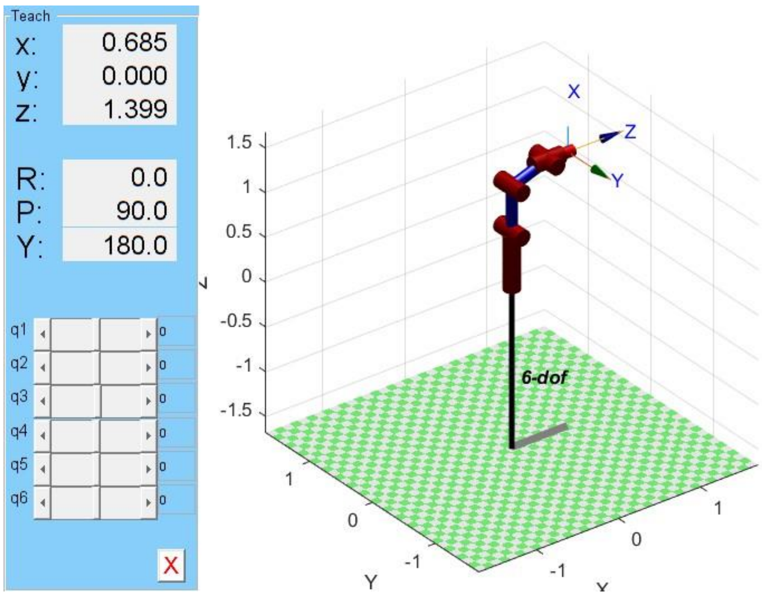

Figure 10. Robotic arm simulation model

5. Robotic arm trajectory planning

Trajectory planning is to prescribe the operation sequence and action process of the robot in advance according to the task requirements [13], and the trajectory planning is divided into joint space and Cartesian space trajectory planning. Firstly, the initial position and target position of the end manipulator should be determined, the initial angle and target angle of each joint should be found out according to the inverse kinematics, the planning should be estimated to find out the angular change curves of each joint, and finally the motion control should be carried out so as to make the robot move according to the results of the trajectory planning.

In this paper, joint spatial planning is used to plan the spatial motion trajectory of the end of the robotic arm by determining the sequence of angle changes of each joint. For the multi-point trajectory planning problem, in order to ensure the smooth operation of the robotic arm, we give the velocity, angle and acceleration of the start and end points, and use the fifth-degree polynomial interpolation to make a smooth continuous curve, i.e.:

$$\theta_t = a_0 + a_1(t-t_s) + a_2(t-t_s)^2 + a_3(t-t_s)^3 + a_4(t-t_s)^4 + a_5(t-t_s)^5 \tag{7}$$

To solve the quintic polynomial, we establish six constraints as the angular displacements, angular velocities and angular accelerations at the start and end points, respectively:

$$\begin{cases} \theta(t_s) \\ \theta(t_e) \\ \dot{\theta}(t_s) \\ \dot{\theta}(t_e) \\ \ddot{\theta}(t_s) \\ \ddot{\theta}(t_e) \end{cases} \tag{8}$$

Solving the system of joint equations gives the fifth-degree polynomial coefficients:

$$\begin{cases} a_0 = \theta_s \\ a_1 = v_s \\ a_2 = 0.5\alpha_s \\ a_3 = \frac{1}{2T^3}[20(\theta_e - \theta_s) - (8v_e + 12v_s)T + (\alpha_e - 3\alpha_s)T^2] \\ a_s = \frac{1}{2T^4}[-30(\theta_e - \theta_s) + (14v_e + 16v_s)T - (2\alpha_e - 3\alpha_s)T^2] \\ a_e = \frac{1}{2T^5}[12(\theta_e - \theta_s) - (6v_e + 6v_s)T + (\alpha_e - \alpha_s)T^2 \end{cases} \tag{9}$$

Through the observation of the actual logistics robotic arm grasping situation, the average grasping time is about 30s, so this paper sets the movement time of 40s, simulates the movement of the robotic arm, and obtains the relative position, angular velocity and angular acceleration trajectory diagrams of the various joints, which are shown in Figures 11-13.

From Figure 11-13, it can be seen that the position, velocity and acceleration of each joint do not differ much. The relative position curves of each joint are basically consistent, smooth and continuous, without sudden changes. The angular velocity of joint 1 increase from 0 to an extreme value and then decreases to 0, while the angular acceleration has two opposite extreme points, increasing from 0 to a great value and then decreasing to 0. The angular velocities of joints 2, 3, 4, 5 and 6 decrease from 0 to an extreme value and then increase to 0, and the angular acceleration has the same two extreme points, decreasing from 0 to a minimum value and then increasing to a maximum value. It shows that the mechanical arm is in a small range of continuous motion form, first accelerated and then decelerated, will not produce sudden shock and vibration. It ensures the smoothness and continuity of the movement of the robotic arm, which meets the needs of the real situation and can be better applied to different scenarios [14].

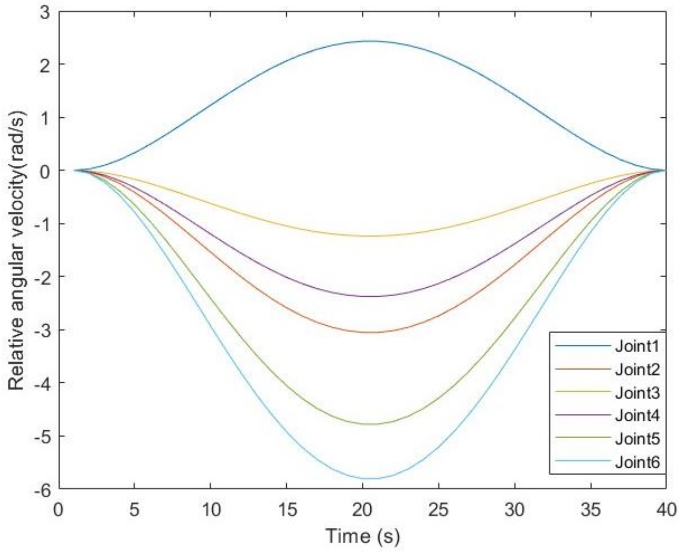

Figure 11. Joint angular velocity diagram

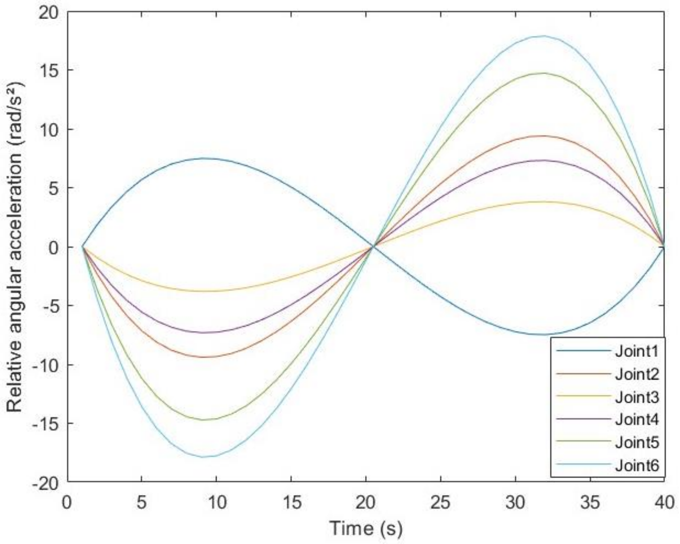

Figure 12. Articular angular acceleration diagram

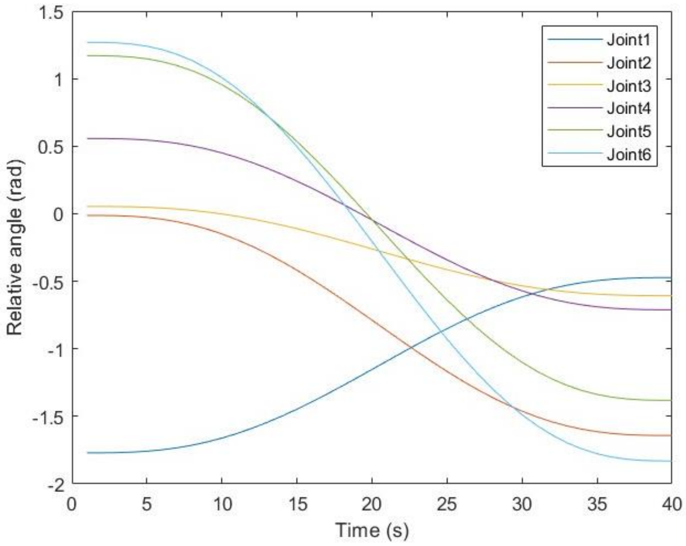

Figure 13. Joint Angle Diagrams

In actual production, the manipulator needs to carry from multiple fixed points to fixed points in this paper, a moving task is designed to set three different starting points of the manipulator, and the objects are placed in three different positions [15]. The vision system obtains the position coordinates of the end points of the manipulator, solves the pose matrix and brings it into the simulation model Trajectory planning of spatial relative position shows the trajectory of end effector motion as shown in Figure 14 By comparing the simulation results of the manipulator, it is proved that the path planning is correct. The manipulator can complete the expected work from point to point according to the set value and realize the target grasping.

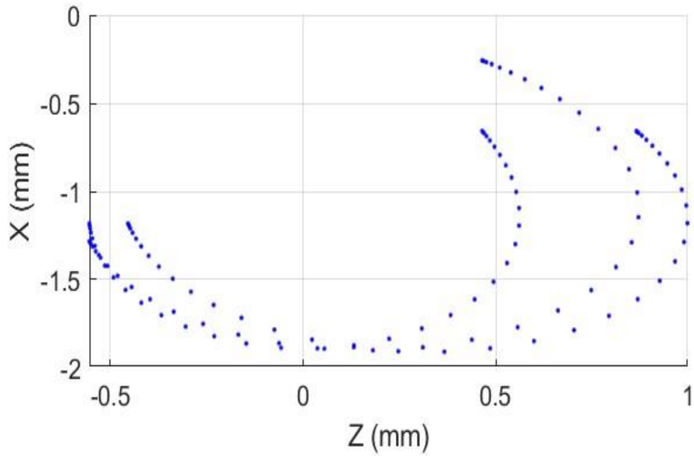

Figure 14. Spatial displacement map

The end effector velocity and angular velocity of the manipulator are also inconsistent at different starting and ending points [16]. See Figure 15.

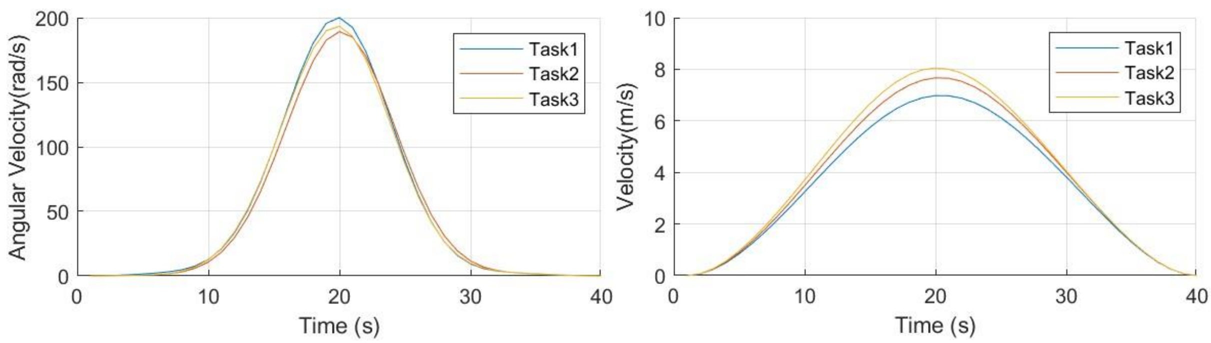

Figure 15. End-effector speed and angular velocity

The angular velocity and velocity of the end effector show curves, which can ensure the stability of grasping objects in actual grasping objects [17]. Grasping objects at a uniform speed prevents the operation efficiency and stability of the mechanical arm.

6. Conclusion

For the research of six-degree-of-freedom robotic arm, this paper establishes a logistics manipulator with visual recognition function. Firstly, the overall structure of the manipulator is made by 3D mapping software, and the 3D model diagram is converted into a 2D motion model diagram. An accurate coordinate system is established for the manipulator arm by improving the D-H parameter method, the coordinates of the target object are recognized by the visual recognition system, and its kinematic equations are derived based on these coordinate systems. The results show that the robotic arm structure with a camera added realizes the function of automatically locating the coordinates of the object and improves the grasping efficiency.

Secondly, a simulation model was constructed for the robotic arm using the toolbox included in MATLAB, and the accuracy and reliability of the model were verified through forward and inverse kinematic analysis. For the kinematic analysis, the fifth-degree polynomial interpolation algorithm was chosen, and this algorithm performs excellently in trajectory planning in the joint space of the robotic arm. The angular, angular velocity and angular acceleration curves of each joint were obtained by analyzing the start and end positions. The results show that the curves are smooth and continuous, showing that the acceleration increases and then decreases without any sudden change in the motion process, which fully proves that the fifth-degree polynomial interpolation method has a better optimization effect in trajectory planning.

Finally, the scene of fixed-point grasping and handling in logistics grasping is simulated, and the coordinates of the initial point and the termination point are set for many times, and the velocity and angular velocity of the end-effector are calculated and the motion trajectory curve of the end-effector is plotted through MATLAB simulation. The comparison of the three results shows that the robotic arm can complete the grasping and handling task with the expected accuracy and stability, and meet the requirements of motion accuracy and smoothness.

The research in this paper provides a theoretical basis for the stable, safe and reliable movement of the manipulator in the operation, and also provides a certain technical support for the application of the manipulator in the actual scene such as logistics operation This research has certain theoretical significance and engineering application value, which lays a foundation for the follow-up research and application of the manipulator.

References

[1] Fu X, Han S, Zhang D, et al. Kinematics and Trajectory Planning of Packaging Sorting Manipulator Based on D-H Method [J]. Packaging and Food Machinery, 2018, 36 (5): 47 - 50.

[2] Zhang Y. Research on Apple Picking with Robotic Arm Based on Deep Learning [D]. Beijing Forestry University, 2020.

[3] GUO W, LI R, CAO C, et al. A New Method for Solving Trajectory Planning and Dynamic Load-Carrying Capacity of a Robot Manipulator [J]. Mathematical Problems in Engineering, 2016, 1302537: 1 - 28. [11] Dong Wen. Structural Design of Picking Manipulator Based on Kinematic Mechanics Model [J]. Agricultural Mechanization Research, 2023, 45 (12): 50 - 53 62.

[4] PARIKH P A, TRIVEDI R R, JOSHI K D. Trajectory Planning of a 5 DOF Feeding Serial Manipulator Using 6th Order Polynomial Method [C]//Journal of Physics: Conference Series, Bristol, 2021.

[5] Wang Z, Du Y, Yang M, et al. Motion Planning of Dobot Robotic Arm Based on MATLAB Robotics Toolbox [J]. Mechanical Research and Application, 2021, 34 (02): 49 - 51.

[6] Jia J, Wang J. Application of Decision Tree Algorithm in Collision Avoidance of Robotic Arms [J]. Mechanical Design and Manufacturing, 2024, (01): 236 - 241.

[7] Jin Z, Hu J, Luo H, et al. Technical Features and Trends of Electromechanical-Hydraulic Integrated Control Robotic Arm [J]. Agricultural Machinery Use and Maintenance, 2022, (02): 51 - 53.

[8] Jizhuo Z, Hongqiang W, Wei L, et al. Kinematic Modelling Analysis and Simulation of 6-DOF Manipulator [J]. Journal of Physics: Conference Series, 2023, 2501 (1):

[9] Yue G, Lijin F, Xuejie J, et al. Research on tolerance optimal allocation method for a 6-DOF series manipulator based on DH-parameters [J]. Proceedings of the Institution of Mechanical Engineers, 2023, 237 (10): 2291 - 2305.

[10] Park F C, Martin B J. Robot Sensor Calibration: Solving AX = XB on the Euclidean Group[J]. IEEE Transactions on Robotics & Automation, 1994, 10 (5): 717 - 721.

[11] Kondo N, Yata K, Iida M, et al. Development of an end-effector for a tomato cluster harvesting robot[J]. Engineering in Agriculture, Environment and Food, 2010, 3 (1): 20 - 24.

[12] Li X, Chen W, Wang Y, et al. Design and Experiment of Cherry Tomato Automatic Harvesting System Based on Cascade Visual Inspection [J]. Journal of Agricultural Engineering, 2023, 39 (01): 136 - 145.

[13] Ma Y, Zeng T, Jiang H. MATLAB-based robotic arm kinematics and trajectory planning [J]. Packaging Engineering, 2023, 44 (03): 187 - 193.

[14] Wen J, Du Y, Qin T, et al. Motion planning and simulation of automatic packaging line based on Dobot manipulator [J]. Packaging Engineering, 2021, 42 (21): 231 - 238.

[15] Zheng T, Liu M. Piecewise interpolation trajectory planning of a manipulator [J]. Mechanical Design and Manufacture, 2020, (03): 261 - 264.

[16] Da Y, Zheng C, Sun M. Improved DH and forward and inverse solution calculation of robot kinematics model [J]. Machinery and Electronics, 2019, 37 (10): 72 - 75.

[17] Li L, Kou Z, Wu J. Design and trajectory planning of six-degree-of-freedom manipulator [J]. Coal Mine Machinery, 2019, 40 (08): 43 - 46.